Journal of the Korean Physical Society, Vol. 62, No. 4, February 2013, pp. 612∼618

Characteristics of a-C/B:H Films from Non-toxic o-carborane Vapor Prepared by Using DC Glow Discharges

Jong-Ho Sun, Hyun-Jong Woo and Kyu-Sun Chung
Department of Electrical Engineering, Hanyang University, Seoul 133-791, Korea and Center for Edge Plasma Science (cEps), Hanyang University, Seoul 133-791, Korea

Suk-Ho Hong*
Department of Electrical Engineering, Hanyang University, Seoul 133-791, Korea and National Fusion Research Institute, Daejeon 305-333, Korea

(Received 31 July 2012, in final form 9 January 2013)

A non-toxic boron-containing material, carborane ($C_2B_{10}H_{12}$), has been utilized to deposit amorphous hydrogenated carbon/boron (a-C/B:H) thin films in helium DC glow discharges. The helium plasma was produced at a target pressure of ∼5 mTorr in the pulsed mode at a duty cycle of 0.375 (3 s on/5 s off) or 0.23 (3 s on/10 s off) by using a filament discharge system connected with a carborane evaporation source. Deposited a-C/B:H thin films were characterized by using variable angle spectroscopic ellipsometry, scanning electron microscopy, Auger electron spectroscopy, and X-ray photoelectron spectroscopy. The a-C/B:H thin films have soft polymer-like characteristics with optical constants of n = 1.65 and k = 10^{-3} at 632 nm, and the B/C ratio inside the bulk was ∼2 for an ∼60% boron contents. The evaporation characteristics of carborane powder under vacuum were also investigated.

PACS numbers: 68.55.Jk, 81.15.Gh
Keywords: Boron, Thin film, Carborane
DOI: 10.3938/jkps.62.612

I. INTRODUCTION

Thin solid films applied to a surface of a substrate can enhance the physical and the chemical properties of the substrate. Plasma-enhanced chemical vapor deposition (PECVD) is a widely used technique for the deposition of insulating films such as silicon-nitride, silicon-oxide, and hydrogenated amorphous carbon films [1–12]. Recently, carbon-boron-containing thin films (C/B films) have gained interest due to their wide variety of physical properties, which is attractive for various applications in, *e.g.*, semiconducting materials [13–15]. The C/B thin films are prepared by using thermal chemical vapor deposition (CVD), bias-assisted hot-filament CVD, ion-beam and electron cyclotron resonance (ECR) plasma-enhanced CVD (PECVD), with boron sources such as BCl_3, B_2H_6, and sputtering of boron and carbon from a target in an N_2 discharge (or boron-nitride). Another interesting functional application of amorphous hydrogenated boron (a-B:H) thin films is for wall conditioning of a nuclear fusion tokamak as an oxygen getter, so-called "boronization". Boronization is a widely and popularly used wall conditioning technique and often utilizes different boron compounds such as diborane B_2H_6 in TEXTOR, DIII-D, and Alcator C-Mod, trimethylboron [$B(CH_3)_3$] in MAST and NSTX, and hydro-decaborane ($B_{10}H_{14}$) in LHD and JT-60. Boronization was found to be efficient to reduce oxygen level in the vacuum vessel [16–22].

One major problem in the fabrication of the boron-containing coatings listed above is the use of toxic and explosive gases: Diborane is a colorless gas at room temperature with a repulsively sweet odor. Diborane mixes well with air, easily forming explosive mixtures. Trimethylboron is a pyrophoric, colorless, and toxic gas. Hydrodecaborane is also toxic. The use of such gases requires strict safety controls and the use of sophisticated protection equipments. On the other hand, solid carborane ($C_2B_{10}H_{12}$) powder is known to be non-toxic and is very easy to handle without severe safety issues [23–28]. Carborane vapor can be produced simply by heating the solid powder in a oven connected to a vacuum vessel, and the flow rate can be regulated by using the oven temperature and a gate valve [27,28]. Therefore, for industrial applications, carborane is attractive as a non-toxic boron source. We have chosen carborane solid powder as the boron source for the deposition of amorphous hydro-

*E-mail: sukhhong@nfri.re.kr; Fax: +82-42-879-5119

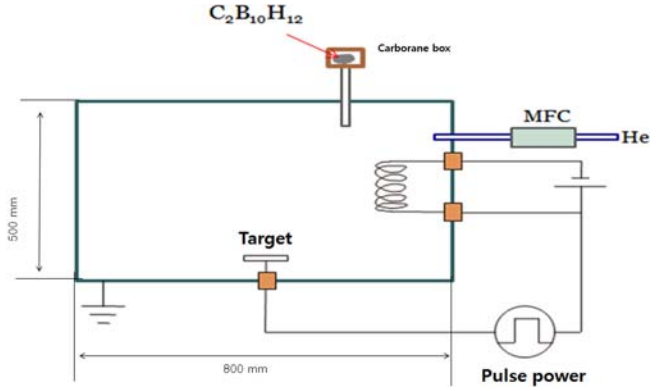

Fig. 1. (Color online) A schematic representation of the experimental chamber.

genated carbon-boron (a-C/B:H) thin films.

In this paper, we report the characteristics of a-C/B:H thin films prepared by using DC glow discharges (GD). In Section II, the experimental setup for the deposition of the a-C/B:H thin films is described in detail, and the diagnostics used to characterize the thin-film properties are introduced. In Section III, the physical and the chemical properties of the a-C/B:H thin films are reported. The results will be discussed in Sec. IV. A conclusion will be given in Sec. V.

II. EXPERIMENTAL SETUP AND DIAGNOSTICS

For the study of evaporation characteristics of carborane vapor under vacuum, a small vacuum chamber with a volume of 0.016 m^3 is utilized. The vacuum vessel has a sample holder on which the carborane solid powder is placed. A vacuum pumping system with a pumping speed of 500 l/s is attached. Through a observation window, the evaporation of the powder is observed and recorded.

A cylindrical vacuum vessel made of stainless steel has been prepared for the reaction chamber. A schematic drawing of the vacuum vessel is depicted in Fig. 1. The vacuum vessel is 800 mm in length and 500 mm in diameter. The volume of the vacuum vessel is 0.16 m^3, with a surface area of 1.26 m^2. A rotary vane and a diffusion pump are used to maintain a base pressure of $\sim 10^{-7}$ Torr with a nominal pumping speed of ∼500 l/s. Helium gas of $5 - 7$ sccm provides a target pressure of $\sim 5 \times 10^{-3}$ Torr for the deposition, but it depends slightly on the condition of diffusion pump. The DC helium discharge is generated by using a DC power supply at a power level of 140 W (V_{DC} = 70 V and I_{DC} = 2 A), which is applied to four tungsten wires of 0.38 mm in diameter. Under these conditions, the plasma density is estimated as $\sim 10^9/cm^3$. For the carborane container and evaporator, an NW25/16KF vacuum component with heater coils and a thermocouple (TZ4L-A4C, TPR-2S) are used. The container is connected to the main experimental chamber through a 1/4 inch tube with a gate valve. The gate valve is used for carborane vapor flow control (injection on/off only). The location of the connection is at 225 mm from one end of the vacuum chamber (Fig. 1). Either 0.5 g or 1 g of carborane is loaded and the carborane container is heated up to 80 °C by using heater coils. Carborane vapor is introduced into the reaction chamber by opening the gate valve after the DC He plasma is generated. To avoid re-condensation of the carborane vapor inside the injection line before it reaches the vacuum vessel [28], we also heat the injection line. P-type (100) silicon wafer pieces are positioned at the bottom of the chamber for the sampling of the thin films. The deposition is performed for about 2 h (total operation time) under a pulsed discharge mode with a duty cycle of 0.375 (3 seconds on and 5 seconds off) or 0.23 (3 seconds on and 10 seconds off).

In order to measure the characteristics of the thin films deposited on the silicon wafers, we have used several analysis tools: A variable angle spectroscopic ellipsometer (Woolam company, VASE) was used to measure the optical constants and the thickness of the film. Because ellipsometry measures the change in the polarization state of light reflected from the surface of a sample, it is a non-intrusive and very sensitive diagnostic. The ellipsometric angles, psi (Ψ) and delta (Δ), are measured as functions of wavelength from 280 to 760 nm at three different angles of incident (65, 70, and 75°)

$$\rho = \frac{R_P}{R_S} = \tan\Psi e^{i\Delta}, \tag{1}$$

where R_P and R_S are the complex reflection coefficients for polarized light. Once Ψ and Δ are measured as functions of wavelength, the thickness and the optical constants are obtained by using a multi-layer model that consists of a silicon wafer as the substrate (1-mm thick), a native oxide layer (SiO_2, 1.5 nm), and a Cauchy layer with Urbach absorption [29]. The chemical composition of the film can be evaluated by using Auger electron spectroscopy (AES) at a sputtering rate of 150 Å SiO_2/min for oxygen. The bonding states of typical elements in films are determined by using an X-ray photoelectron spectroscopy (XPS, PHI 5800 ESCA) with a resolution of 0.48 eV, a beam spot size of 400 × 400 μm^2 and an anode power of 250 W (10 kV, 27 mA). The sputtering rate is 2.5 min/cycle for a 3-keV argon ion beam. The surface morphology is investigated by using scanning electron microscopy (SEM: model CX-100S) and atomic force microscopy (AFM: Park systems).

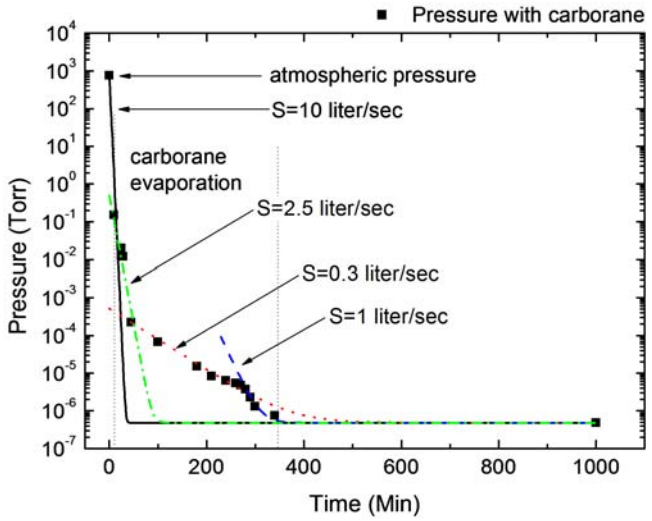

Fig. 2. (Color online) Vacuum vessel pressure as a function of pumping time with an exponential fitting for the determination of the effective pumping speed.

III. RESULTS

1. Evaporation of Carborane Solid Powders Under Vacuum Without a Plasma

Many physical and chemical properties of carborane are still unexplored. If carborane solid powders are to be utilized for PECVD, their behaviors under vacuum have to be known. For this reason, we observe the evaporation characteristics of carborane powder under vacuum at different pressure in a small vacuum chamber. Note that we cannot measure the mass change of the carborane powder in-situ. Instead, we calculate the number of carborane atoms pumped out by measuring the change in pressure for the known volume of the vacuum vessel (0.016 m^3). At first, we load 1 g of carborane at atmospheric pressure (without pumping) and observe it for 3 days at room temperature. No visible change in mass is observed, indicating that the evaporation of carborane at atmospheric pressure at room temperature is negligible. Then, we load 1 g of carborane into the vacuum vessel, and reduce the pressure by pumping. Figure 2 shows that the vacuum vessel pressure decreases as a function of pumping time. Closed squares indicate the measured pressure while the solid, dotted, and dashed lines are from the pressure calculation for different pumping speed:

$$P = P_\infty + P_0 \exp(-\frac{s}{v}t), \tag{2}$$

where P is the pressure inside the vacuum vessel, P_∞ is the final base pressure of 4.8×10^{-7} Torr, S is the effective pumping speed and V is the volume of the vacuum vessel. The pumping speed S of helium is determined by using

$$S_{gas} = S_{N_2}\sqrt{\frac{M_{gas}}{M_{28}}}, \tag{3}$$

where S_{gas} is the pumping speed of a gas, S_{N_2} is the nominal pumping speed, and M_{28} and M_{gas} are the masses of the N_2 molecule and the gas molecule, respectively.

Four different pumping stages are observed. At the beginning of the experiment, the vacuum vessel is closed from the vent at atmospheric pressure: Most of the gas species inside the vacuum vessel, except the loaded 1 g of carborane, is N_2, and the effective pumping speed calculated from the pressure drop is equal to 10 l/s. The effective pumping speed is changed to 2.5 l/s at a pressure of $\sim 1.5 \times 10^{-1}$ Torr, indicating the start of the evaporation of carborane. At pressures from 5×10^{-2} down to 5×10^{-4} Torr, the pressure decreases slowly at a pumping speed of 0.3 l/s due to strong evaporation of carborane molecules. The pumping speed is then changed to 1 l/s and remains constant afterwards. One gram of carborane is fully evaporated after about 340 min under vacuum. The lesson from this experiment is that carborane solid powder starts to evaporate under vacuum condition at 5×10^{-2} Torr, and evaporates more actively at pressures under 5×10^{-4} Torr. This is another reason (other than flow rate control) for the gate valve in front of the carborane container: For the deposition of an a-C/B:H thin film, carborane should be loaded before the experiments, and the gate valve should remain open while pumping down to less than 5×10^{-2} Torr, then closed. The gate should be opened only when the target pressure for the deposition is reached and after the He glow discharge is on.

2. Thickness Profiles and Optical Properties of a-C/B:H Thin Films

The thickness profiles of a-C/B:H thin films deposited at a pressure of 5×10^{-3} Torr by using 0.5 g of evaporated carborane with two different duty cycles are depicted in Fig. 3(a). Silicon wafers are positioned at nine different locations inside the vacuum vessel. The thickness profiles show the effect of the duty cycle. In the case of films deposited with a duty cycle of 0.375 ("375" samples), the film thickness is in a range from 40 to 611 nm while the thickness of films deposited with a dust cycle of 0.230 ("230" samples) is in a range from 109 to 483 nm. "375" samples have their maximum thickness at the position of the anode due to the dense concentration of carborane vapor (near the injection port) and high ionization/dissociation rate near the anode. The thickness of the film decreases almost linearly as the distance from the anode increases in both directions. On the other hand, increasing the plasma off time provides more diffusion time for the evaporated carborane vapor, leading to a "more homogeneous" distribution inside the vacuum

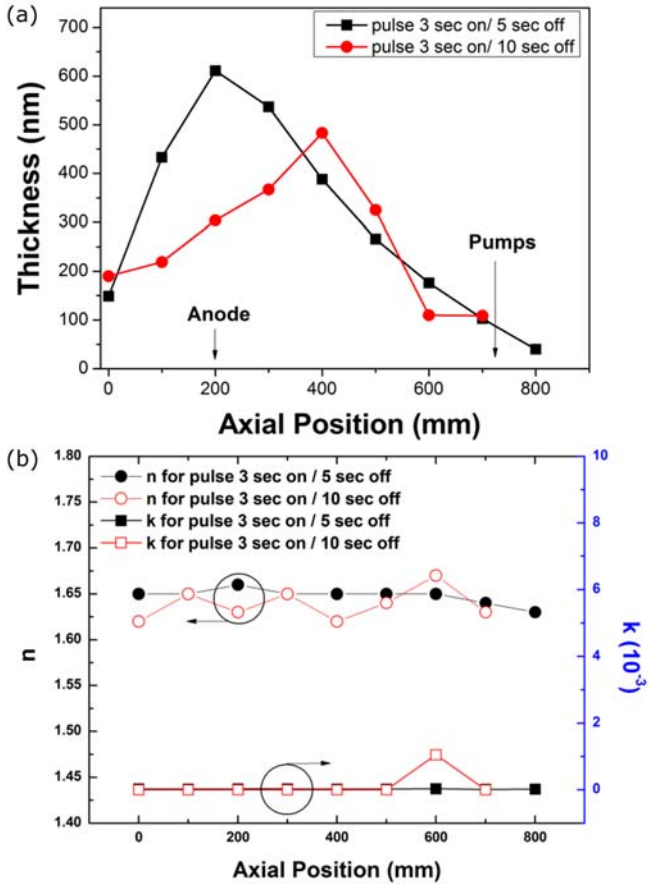

Fig. 3. (Color online) (a) Thickness profiles of a-C/B:H thin films deposited at a pressure of 5×10^{-3} Torr by using 0.5 g of evaporated carborane with two different duty cycles. (b) Optical constants of the films with two different duty cycles.

chamber. However, the diffusion distance is rather limited by pumping: For axial positions larger than 400 mm distance, the duty cycle doesn't much affect the thickness profile: The peak of the thickness profile of "230" samples is shifted towards the pump position, after which the thickness decreases further in a manner similar to that for the "375" samples.

The optical constants of the films are almost the same, meaning that the physical properties and the chemical bonding structures of the films are almost identical (Fig. 3(b)): The index of refraction n and the extinction coefficient k at a wavelength of 632 nm are 1.65 and 10^{-3}, respectively. From a simple scratch test with a needle, the thin film shows soft polymer-like characteristics.

3. Chemical Composition and Bonding Structures of a-C/B:H Thin Films

The depth profile of the atomic composition is measured by using AES coupled with an oxygen beam sput-

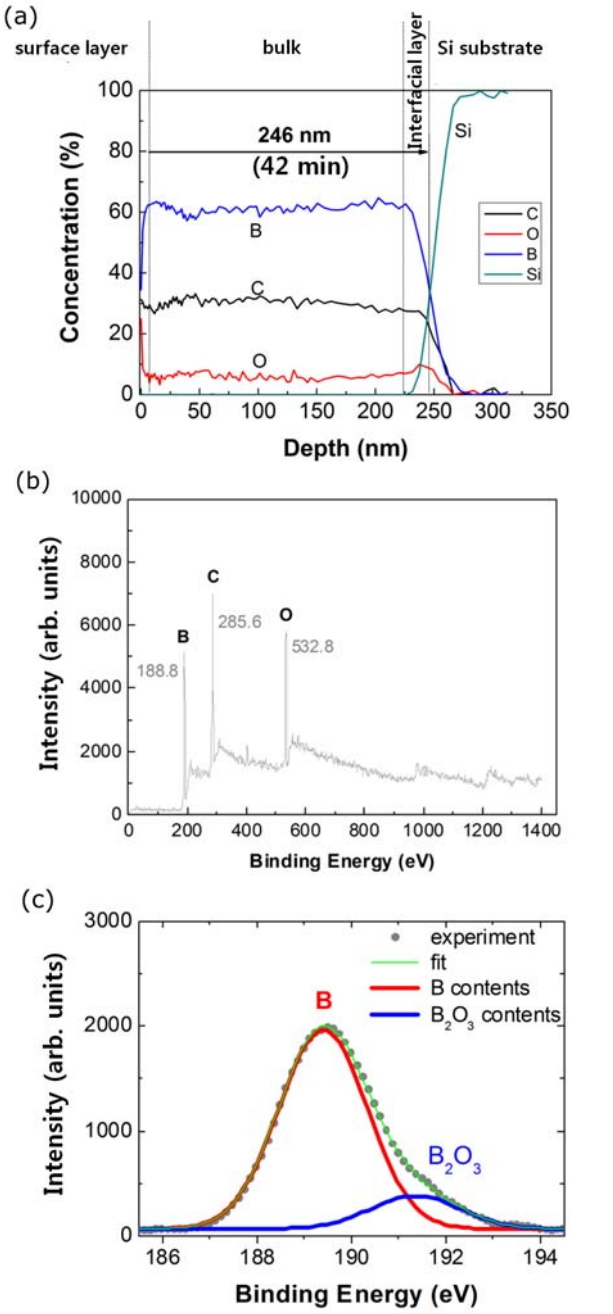

Fig. 4. (Color online) (a) Atomic concentrations of the thin films deposited using 0.5 g of carborane. (b) Typical binding energy spectrum of an a-C/B:H thin film and (c) narrow scan of the boron peak at 188.8 eV.

tering system. The atomic concentrations of the thin films deposited using 0.5 g of carborane are shown in Fig. 4(a). Since the sputtering time is proportional to the thin film thickness, the increase in the silicon peak indicates the presence of an interfacial layer between the bottom of the deposited film and the silicon substrate. Three different regions can be identified as shown in Fig. 4(a): From the silicon substrate in the direction of the surface

layer, the amount of oxygen increases slightly due to the presence of the native silicon oxide layer (∼1.5 nm). The boron and the carbon contents increase rapidly inside the bulk film with atomic ratios of ∼60% boron, ∼30% carbon, and ∼7% oxygen. At the surface layer, plenty of oxygen exists due to surface contamination by moisture. The typical AES spectra of a-C/B:H films do not depend on the thickness of the film. Thicker films of "230" and "375" samples are also examined, and the atomic ratio of B/C is ∼2 regardless of the thickness or depth of the films, or the amount of carborane used for the deposition. This is also consistent with the constant optical properties of the films measured by using spectroscopic ellipsometry, as mentioned above. The film quality is almost constant.

The XPS scan presented in Fig. 4(b) shows typical binding energy spectra for an a-C/B:H thin film including the boron, carbon and oxygen peaks corresponding to binding energies of 188.8, 285.6, and 532.8 eV, respectively [30]. The boron peak at 188.8 eV has a shoulder at a slightly higher energy of 192 ∼ 193.3 eV which is related to B_2O_3 as shown in Fig. 4(c) [31]. Boron forms strong chemical bonds with oxygen to form B_2O_3. From the AES results in Fig. 4(a), the atomic concentrations of B and O inside the bulk a-C/B:H thin film is almost constant, indicating that a constant amount of water is present during the deposition. This reveals an imperfection in the vacuum vessel sealing. Otherwise, the oxygen concentration would decrease down to zero as the thickness of a-C/B:H thin film increases. Then, the oxygen contents increase sharply at the surface due to air exposure. This oxygen gettering function of boron atoms during the deposition process is utilized in many nuclear fusion machines for "thin-film-based wall conditioning" to remove oxygen from the vacuum vessel [16].

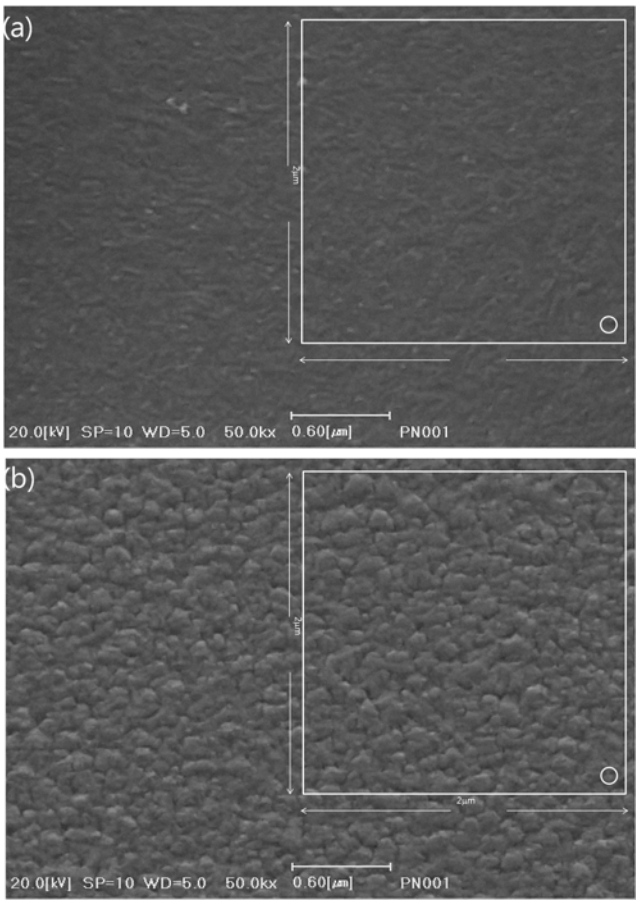

Fig. 5. Evolution of the surface roughness with different amounts of carborane vapor observed by using SEM with 50 k magnifications: (a) 246 and (b) 382 nm.

4. Surface Morphology of a-C/B:H Thin Films

Figure 5 shows the evolution of the surface roughness of a-C/B:H thin films with different amount of carborane vapor observed by using SEM with 50 k magnification. The thicknesses of the films in Fig. 5 are (a) 246 and (b) 382 nm, respectively. A clear difference in the surface morphology is observed: The surface structure of the thinner film is in a developing phase so that the surface is relatively flat with some small surface structures. On the other hand, the thicker one shows a "fully-developed" surface structure with a surface roughness of ∼7 − 8 nm. The size of the surface structures is around 100 nm (circles in Fig. 5) or a bit larger.

The surface structure of the films is measured (2 μm × 2 μm) and analyzed by using AFM as shown in Fig. 6. As we have seen from the SEM images (see rectangles in Fig. 5, 2 × 2 μm), the thinner one shows rather a flat surface while the thicker one shows a dot-like structure with an average height of 7.5 nm. The size of the dot-like structures are about 80 − 100 nm in diameter, which is consistent with the SEM measurements. Note that the rectangles in Fig. 5 are only guides for comparison and do not mean we have measured the specific positions by using AFM: we have measured the surface profiles at near locations.

IV. DISCUSSION

The evaporation characteristic of carborane solid powder in Fig. 2 indicates that the evaporation of carborane at pressures higher than 5×10^{-4} Torr is small compared with that at pressures below 5×10^{-4} Torr, which suggests that the operation range for the He DC glow discharge for the deposition of a-C/B:H thin films should be higher than 5×10^{-4} Torr: Deposition at this pressure level leads to much faster consumption of source material; thus, it is economically not suitable.

Deposited films show polymer-like (soft) characteristics: The optical constants of the films at different locations are identical. Surface roughness evolves with the

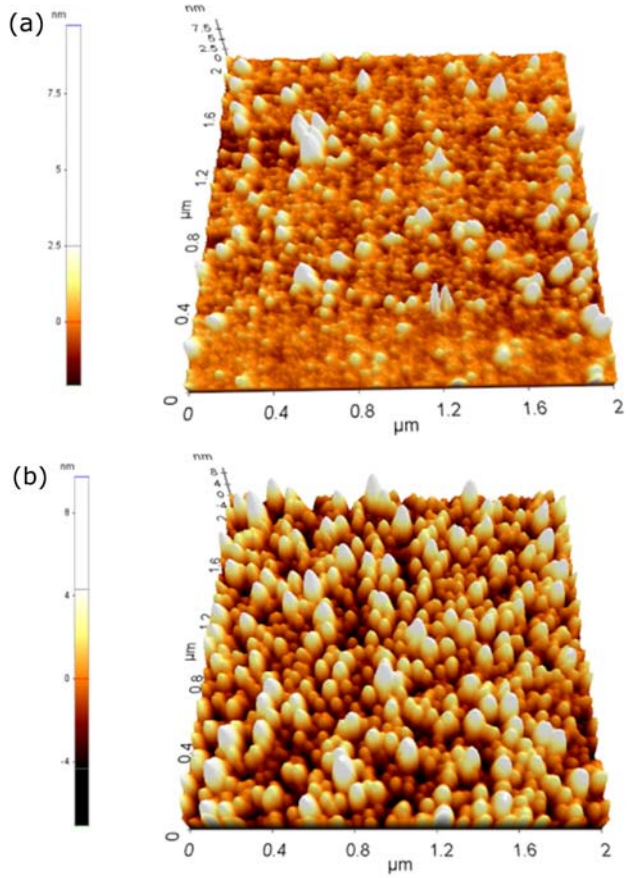

Fig. 6. (Color online) The surface structure of the films measured (2 μm × 2 μm) and analyzed by using AFM: (a) 246 and (b) 382 nm.

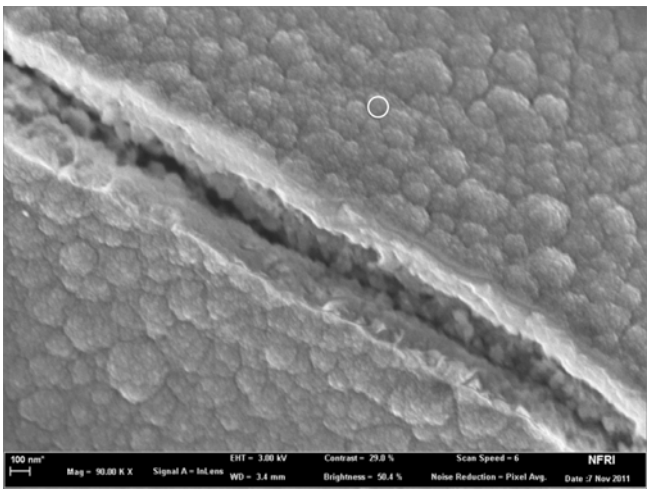

Fig. 7. FE-SEM image of the 382 nm film.

thickness of the film. Furthermore, the evolution of the surface structure shows a cauliflower-shaped fine structure as shown in Fig. 7 imaged with a magnification of 90 k. The circle in Fig. 7 is 100 nm in diameter, and much smaller surface structures can be clearly seen. The only difference among the films is the thickness. This indicates that the deposition was dominated by low energy ions, radicals, and neutrals. Furthermore, the deposition occurs at the backside of the silicon wafer (not shown here). This tell us that carborane or cracked carborane components have a low sticking coefficient, which leads to deposition even at the shadow, which cannot occur during an ion-dominated deposition.

V. CONCLUSION

In this paper, we have utilized a carborane solid powder, which is not toxic and easy to handle, to deposit boron-containing thin film on silicon wafers by using helium DC glow discharge. This experiment shows the possibility of depositing boron-containing thin films by using a non-toxic and safe material.

The deposited boron-containing films have (soft) polymer-like thin film characteristics with cauliflower-shaped surface structure, and the surface roughness has evolved with the thickness. Other physical characteristics of the films were affected by neither the position inside the vacuum chamber nor the duty cycle, which was due to the deposition mechanism being dominated by low energy ions, radicals, and neutrals.

ACKNOWLEDGMENTS

This research was supported by the National R&D Program through the National Research Foundation of Korea (NRF) funded by the Ministry of Education, Science and Technology (20110018734).

REFERENCES

[1] B. Gorowitz, T. B. Gorczyca and R. J. Saia, Solid State Technol. **28**, 197 (1985).
[2] T. I. Kamins and K. L. Chiang, J. Electrochem. Soc. **129**, 2326 (1982).
[3] J.-J Hajjar, R. Reif and D. Adler, J. Electron. Mater. **15**, 279 (1986).
[4] S. Suzuki and T. Itoh, J. Appl. Phys. **54**, 1466 (1983).
[5] J. H. Comfort, L. M. Garverick and R. Reif, J. Appl. Phys. **62**, 3388 (1987).
[6] K. P. Pande and A. C. Seabaugh, J. Electrochem. Soc. **131**, 1357 (1984).
[7] Y. Dachuan, X. Niankan, L. Zhengtang, H. Yong and Z. Xiulin, Surf. Coat. Technol. **78**, 31 (1996).
[8] M. Maharizi, O. Segal, E. Ben-Jacob, Y. Rosenwaks, T. Meoded, N. Croitoru and Seidman, Diamond Relat. Mater. **8**, 1050 (1999).
[9] M. Schreck, T. Baur, R. Fehling, M. Muller, B. Stritzker, A. Bergmaier and G. Dollinger, Diamond Relat. Mater. **7**, 293 (1998).

[10] R. Gago, O. Sanchez-Garrido, A. Climent-Font, J. M. Albella, E. Roman, J. Raisanen and E. Rauhala, Thin Solid Films **338**, 88 (1999).
[11] S. Yugo, N. Ishigaki, K. Hirahara, J. Sano, T. Sone and T. Kimura, Diamond Relat. Mater. **8**, 1406 (1999).
[12] M. Zarabiab, N. Fourches-Coulon, G. Turban, M. Lancin and C. Marhic, Diamond Relat. Mater. **6**, 542 (1997).
[13] B. G. Bagley, D. E. Aspnes, A. C. Adams and R. E. Benenson, J. Non-Cryst. Solids **35**, 441 (1980).
[14] K. Shirai and S. Gonda, J. Appl. Phys. **67**, 6286 (1990).
[15] N. Bernhard *et al.*, in *Amorphous Silicon Technology - 1991 Symposium* (Materials Research Society, New York, 1991), p. 289.
[16] J. Winter *et al.*, J. Nucl. Mater. **162**, 713 (1989).
[17] G. L. Jackson *et al.*, Phys. Rev. Lett. **3098**, 67 (1991).
[18] M. Greenwald *et al.*, Nucl. Fusion **793**, 37 (1997).
[19] A. Sykes *et al.*, Nucl. Fusion **1423**, 41 (2001).
[20] C. H. Skinner *et al.* Nucl. Fusion **329**, 42 (2002).
[21] Y. Nobuta *et al.*, Fusion Eng. Des. **81**, 187 (2006).
[22] M. Saidoh *et al.*, Fusion Eng. Des. **271**, 22 (1993).
[23] V. M. Sharapov *et al.*, J. Nucl. Mater. **220**, 730 (1995).
[24] J. Li *et al.*, Nucl. Fusion **39**, 973 (1999).
[25] X. Gao *et al.*, J. Nucl. Mater. **390**, 864 (2009).
[26] D. Tafalla *et al.*, Vacuum **67**, 393 (2002).
[27] O. I. Buzhinskij *et al.*, J. Nucl. Mater. **313**, 214 (2003).
[28] S. H. Hong *et al.*, Nucl. Fusion **51**, 103027 (2011).
[29] C. Herzinger *et al.*, *Guide to Using WVASE32* (J.A. Woollam, Lincoln, USA, 1999).
[30] *Thermofisher Scientific*, http://www.lasurface.com.
[31] A. Yoshikawa *et al.*, J. Nucl. Mater. **367**, 1527 (2007).